# Multichannel 3D Ground Penetrating Radar – Advances in Civil Infrastructure Scanning

**Lee Tasker**
*University of Western Australia*
*School of Civil, Environmental and Mining Engineering*
*35 Stirling Highway, Crawley, Perth, WA 6099*
*lee.tasker@uwa.edu.au*

**Kathleen L. McMahon**
*Draig Geoscience Pty. Ltd.*
*13/11 Milson Place, O'Connor, WA 6163*
*kath@driaggeoscience.com*

## SUMMARY

The scope of this paper is to highlight improvements in Ground Penetrating Radar (GPR) as an infrastructure condition assessment tool, in particular through the use of multichannel 3D GPR.

Multichannel 3D GPR is a relatively new and alternative infrastructure scanning tool which can assist geophysicists and engineers in providing 100% sub-surface coverage of an investigation area, where site access is possible. Advantages of an increased level of subsurface coverage using multichannel 3D GPR includes providing the user with improved accuracy in highlighting and quantifying regions that may require further invasive testing for future maintenance programs and also possible long-term monitoring.

This paper briefly discusses current applications of standard GPR for infrastructure condition assessments and how multichannel 3D GPR can improve knowledge of the sub-surface in these application areas.

Visualisations of multichannel 3D GPR data outputs with interpretations have been presented to illustrate the improved subsurface information made available from this method. The example presented is an approximately 4 m long section of multichannel 3D GPR data acquired along the surface of a reinforced concrete-lined tunnel.

**Key words:** Multichannel 3D Ground Penetrating Radar, 3D GPR, Infrastructure Scanning, Tunnel Lining, Condition Assessment, Condition Monitoring.

## INTRODUCTION

Multichannel 3D GPR is a relatively new geophysical method. 3D GPR is widely used for many applications such as road condition assessments (Muller, 2012), bridge deck condition inspections (Tarussov *et al.*, 2013), archaeological prospecting (Trinks *et al.*, 2010) and for buried services and utility locating (Zarkhidze and Lemenager, 2004).

The application of multichannel 3D GPR for scanning the subsurface of vertical or non-planar civil infrastructure (e.g. walls, tunnels and bridge abutments), in a manner where the GPR signal is not directed down into the ground, is uncommon.

Primarily, high frequency (400 MHz to 2 GHz) 2D GPR is the standard methodology for scanning the subsurface of civil infrastructure. Barrile and Pucinotti (2005) provide some example applications for standard GPR civil infrastructure investigations:

(i) Estimation of thickness elements from one surface;
(ii) Localisation of reinforcing bars and metallic ducts, and estimation of rebar size;
(iii) Estimation of the concrete cover depth;
(iv) Localisation of moisture variations;
(v) Localisation and dimension of voids/cavities;
(vi) Localisation of cracking;

Currently many 3D GPR interpretations of civil infrastructure are produced by creating a 3D image reconstruction of multiple densely spaced 2D GPR profiles, which are used to locate possible areas of subsurface interest (Topczewski and Fernandes *et al.,* 2007). This 3D GPR method extends the diagnostic ability of 2D GPR and assists in providing a more detailed image of the sub-surface, as Stainbruch (2009) has shown in a study of a concrete reinforced water tunnel in Prague.

Accurate positioning of the 2D profiles in relation to each other is important. An issue with using 2D profiles to create 3D image reconstructions is that errors in profile positioning lead to possible errors or artifacts in 3D reconstructions. Stainbruch (2009) states that multichannel 3D GPR allows for a finer resolution of data and provides a more accurate method of data positioning in comparison to multiple hand-held GPR profiles.

This paper discusses multichannel 3D GPR data acquired along the lining surface of a tunnel. With multichannel 3D GPR, it is possible to collect a swath of data in a single pass. The centres of the multichannel antennas in this case study were spaced 4.5 cm apart, which is a much closer profile spacing that is generally possible with standard 2D profiles. As well as multichannel 3D GPR providing a more detailed and accurately located GPR image than 3D image reconstructions of 2D GPR

profiles, or indeed 2D GPR profiles alone, the acquisition of 3D GPR data using a multichannel 3D GPR system is also more time efficient. The requirement of collecting multiple densely spaced 2D profiles is made redundant, as in this example acquiring a 1 m swath of data with fixed antenna separation of approximately 4.5 cm is possible with a pass.

## METHOD AND RESULTS

The example presented here is an approximately 4 m long section of multichannel 3D GPR data, acquired along the surface of a reinforced concrete-lined tunnel. At this location a crack within the concrete was visible at the surface.

The data was acquired using the MALÅ Imaging Radar Array (MIRA) 1.3 GHz multichannel system, with 12 transmitters and 11 receivers in an offset array within an approximate total swath width of 1 m. The spacing between each transmitter-receiver pairing was approximately 4.5 cm. A record length of 21.5 ns was used with a sample frequency of approximately 20 GHz.

The MALÅ proprietary software rSlicer (v 2.1.1001) was utilised to process the multichannel 3D GPR data, producing a 3D volume of GPR data. Processing steps applied to the data include zero-time correction, filtering, migration and post-migration filtering.

The resultant 3D GPR data volume is able to be viewed as planar depth slices (from the surface into the volume), and as cross-sections cut at any angle through the data volume. Examples of selected depth slice images from the surface of the tunnel lining through to 36.70 cm depth are displayed in Figure 1. An example cross-section of the data, from the surface into the tunnel lining is shown in Figure 2. This cross-section is cut perpendicularly to the reinforcement bars (rebar).
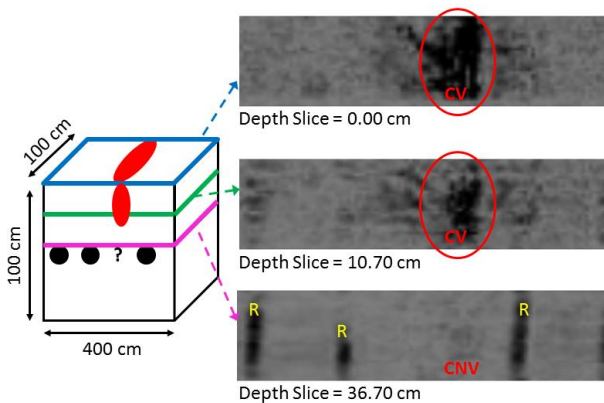


**Figure 1.** **Example 3D GPR data "slice" views of an interpreted crack location within a reinforced concrete wall. Data slices showed at three different depths into the wall: 0.00 cm, 10.70 cm and 36.70 cm. CV = crack visible, CNV = crack not visible, R = reinforcement bar (rebar).**
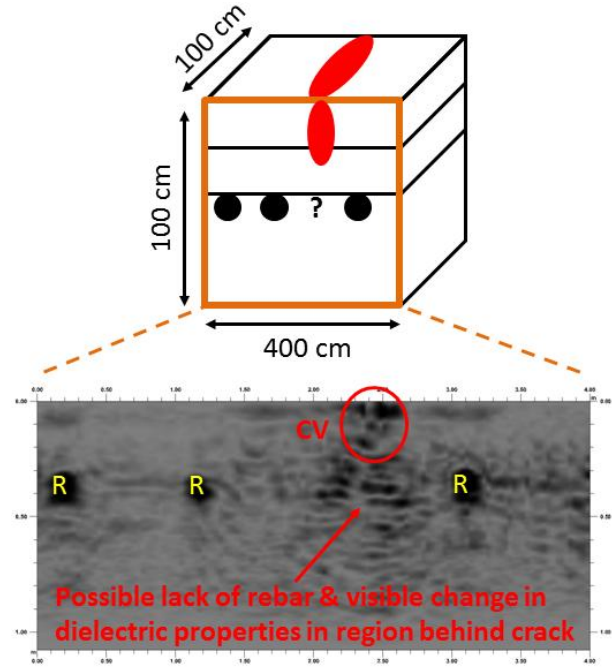


**Figure 2.** **Example 2D GPR data cross-section visualisation from the 3D GPR data set shown in Figure 1; 2D cross-section through a reinforced concrete wall. CV = crack visible, R = reinforcement bar (rebar).**

Within the Figure 1 depth slice images, a noticeable GPR response is observed at the crack location at the surface (0 cm depth). A similar GPR response continues to a depth of at least 10.70 cm, however by 36.70 cm it is no longer visible. The GPR response of the crack feature can be interpreted at each depth slice, giving a 3D location including a quantification of dimensions and a 3D representation of the shape.

Within the cross-section in Figure 2, the identifiable GPR response extending from the surface crack location is also observed to extend to >10.70 cm, however cannot be clearly identified at the depth of the observed rebar. The region of data at depth below the crack location displays a change in response compared to the areas adjacent where no surface crack is visible. This may be due to a change in dielectric properties in this region, or is a data effect of the strong near-surface responses.

The 3D GPR data has revealed the presence of rebar within the tunnel lining, encountered from a depth of approximately 36.70 cm. Three vertical bar-shaped features are identified. The difference in the vertical length of the rebar features in the 36.70 cm depth slice image in Figure 1 is likely due to local differences in the angle and positioning of the rebar. It is also observable that the distance between rebar is inconsistent, with a closer spacing between the first and second bars (from left to right) and a distance approximately double this between the second and third bars. Noticeably it is in this same location where a larger gap in rebar is observed that a crack is present at the tunnel lining surface, and where the interpreted crack in the GPR data extends into the tunnel lining.

## CONCLUSIONS

In summary, positioning of data is crucial in the acquisition phase for later location of interpreted features. Multichannel 3D GPR acquisition allows for improved positioning due to the constant relative positions of the multiple transmitters and receivers. The utilisation of multichannel 3D GPR data acquisition also removes the pre-planning requirement in 2D GPR investigations to orient survey lines perpendicular or oblique, rather than in-line, with linear structures or features. In this way, multichannel 3D GPR allows for improved blind testing of sites.

Reconstructed 3D imaging of 2D profiles lead to artefacts interpolated between GPR profile data. Similarly, more than one interpretation may fit a manual interpolation of features between 2D profiles. Multichannel 3D GPR improves the level of detail for subsurface investigations of civil infrastructure by revealing an accurate 3D representation of the subsurface.

Within the presented multichannel 3D GPR tunnel data results, at the location of an observed surface crack a GPR response for this feature was identified and interpreted to depth within the tunnel lining. The multichannel 3D GPR results allow for measurement and quantification of crack dimensions, shape and orientation, which is an improvement over standard 2D GPR profile interpretation. By observing GPR responses at known crack locations, the data can be examined for similar features to identify possible crack features at locations where a crack is not yet visible at the tunnel surface. The multichannel 3D GPR data has also provided information on the presence (or lack of), localisation and orientation of reinforcement bars. Notably, in this case the location of the visible crack and the interpreted GPR crack feature at depth coincides with the lack of an observed rebar.

Multichannel 3D GPR is a viable tool for 4D monitoring of civil infrastructure over time, either for new infrastructure or aging infrastructure. A baseline GPR dataset may be compared to subsequent GPR datasets for the same location, identifying and quantifying the development or progression of infrastructure fatigue or degradation.

**REFERENCES**

Barrile, V. and Pucinotti, R., 2005, Application of radar technology to reinforced concrete structures: a case study, NDT & E International, 38(7), 596-604.

Muller, W., 2012, A network-level road investigation trial using Australian-made traffic-speed 3D Ground Penetrating Radar (GPR) technology. 25th ARRB Conference - Shaping the future: Linking policy, research and outcomes. Perth, Australia, ARRB Group Ltd.

Stainbruch, J., 2009, The GPR scanner as the next step in detailed 3D diagnostics, Defektoskopie, 39th Conference and Exhibition, Prague, Czech Republic.

Tarussov, A., Vandry, M., De La Haza, A., 2013, Condition assessment of concrete structures using a new analysis method: Ground-penetrating radar computer-assisted visual interpretation, Construction and Building Materials 38: 1246-1254.

Topczewski, L., Fernandes, F.M., Cruz, P.J.S., Lourenço, P.B., 2007, Practical implications of GPR investigation using 3D data reconstruction and transmission tomography, Journal of Building Appraisal, 3(1), 59-76.

Trinks, I., Johansson, B., Gustafsson, J., Emilsson, J., Friborg, J., Gustafsson, C., Nissen, J., Hinterleitner, A., 2010, Efficient, large-scale archaeological prospection using a true three-dimensional ground-penetrating Radar Array system, Archaeological Prospection, 17(3), 175-186.

Zarkhidze, A., Lemenager, E., 2004, Case study - use of 3D GPR technologies for utility mapping in Paris, 10th International Conference on GPR, Delft, The Netherlands, 375-378.